Bol. Soc. Paran. Mat.
©SPM – E-ISSN-2175-1188
SPM: www.spm.uem.br/bspm

(3s.) **v. 2025 (43) 4** : 1–15.
ISSN-0037-8712
doi:10.5269/bspm.78578

Natural Convection Flow of Magnetohydrodynamic Micropolar Fluid in a Dome-Shaped Enclosures

Gandrakota Kathyayani*, Siddamsetti Maheswari and Gattu Venkata Ramudu

ABSTRACT: This study conducts a numerical investigation into laminar flow and natural convection heat transfer of micropolar fluid within dome-shaped enclosures (DSEs). The enclosure features adiabatic left and right walls, while the bottom wall is maintained at constant temperatures, with top dome-shape wall is cold. The study examines how the unique geometry of DSEs influences natural convection (N.C.) and flow characteristics under varying parameters such as Rayleigh number (Ra), Prandtl number (Pr), Hartmann number (Ha), micropolar parameter (K), and radiation parameter (Rd). The developed mathematical model, based on the vorticity-stream function method, investigates the influence of magnetic field strength and direction, micropolar fluid characteristics, and radiative heat transfer on both thermal and flow behavior. The results reveal significant modifications in velocity profiles, temperature distribution, and microrotation patterns due to changes in magnetic and radiative effects. This comprehensive analysis contributes to a deeper understanding of MHD natural convection in micropolar fluids with thermal radiation, aiding progress in advanced heat management systems and industrial applications.

Key Words: Dome-shaped enclosure, micropolar fluid, stream function–vorticity formulation, magneto-hydrodynamic, thermal radiation, finite difference method.

Contents

1 Introduction **1**

2 Mathematical Formulation **3**

3 Numerical methodology and code validation **5**

4 Results and Discussion **5**

5 Conclusions **12**

1. Introduction

Due to its importance in a variety of engineering and industrial applications, such as thermal insulation, electronic device cooling, and energy storage systems, natural convection in enclosures has been extensively researched.When dealing with micropolar fluids−fluids with microstructure effects that exhibit microrotation and spin−flow behavior becomes significantly different from that of conventional Newtonian fluids. The incorporation of a magnetic field further influences the dynamics, making magnetohydrodynamic (MHD) natural convection an important subject in fluid mechanics.

Micropolar fluids, introduced by Eringen (1966), represent a class of complex fluids that incorporate microstructural effects, including microrotation and microinertia. These fluids differ from standard Newtonian fluids in that they are composed of stiff, randomly oriented (or spherical) particles floating in a viscous medium. Micropolar fluids are widely used in applications such as lubrication, polymer processing, biological flows, and plasma physics, where the internal structure of the fluid plays a significant role in its behavior. The governing equations of micropolar fluids extend the Navier-Stokes equations by incorporating additional terms that account for the spin and micro-rotational effects. [1] explored the heat transfer characteristics of a micropolar fluid under the influence of thermal radiation. Their study provided fundamental insights into how radiation modifies convective heat transfer, emphasizing the reduction in heat transfer rates due to radiative losses. This work was expanded by [2] by taking into account the natural convection of a micropolar fluid inside a porous square conduit, taking into account

* Corresponding author.
2010 *Mathematics Subject Classification:* 35B40, 35L70.
Submitted August 22, 2025. Published October 09, 2025

the effects of thermal radiation, heat generation/absorption, and a magnetic field. Their findings showed that while thermal radiation improves the homogeneity of the temperature distribution, an increase in the Hartmann number (Ha) reduces convective motion. Using the boundary element approach, [3] examined the natural convection of a micropolar fluid in an enclosure. They emphasized how important micropolar factors are for altering heat transfer rates and flow dynamics. Similarly, [4]investigated natural convection in a differentially heated enclosure and found that because of the microstructure's resistance to fluid motion, micropolar fluids transport less convective heat than Newtonian fluids. An earlier study by [5] analyzed micropolar convection in a rectangular enclosure, concluding that both the Rayleigh number (Ra) and micropolar parameters significantly affect the heat transfer process. [6] further studied natural convection in enclosures with discrete heaters, demonstrating that localized heating alters flow circulation and heat transfer patterns significantly. In a computational investigation of micropolar flow within a lid-driven triangular enclosure, [7] demonstrated how enclosure geometry affects heat transmission and flow behavior. In order to change convection dynamics, [8] examined mixed convection in a triangular cavity filled with a micropolar nanofluid-saturated porous media, highlighting the interplay between MHD and micropolar effects.

Recent studies have expanded on these findings by incorporating nanofluids and complex geometries. [9] examined the impact of nanoparticle shape factors on double diffusive convection in a trapezoidal porous enclosure, revealing significant alterations in heat and mass transfer rates. [10] demonstrated the interaction between magnetic forces and convective currents by simulating natural convection in a porous enclosure filled with magnetic nanofluid using Buongiorno's two-component model. The impact of thermal radiation on convection in a trapezoidal enclosure was previously investigated by [11], who focused on heat flow visualization through the use of energy flux vectors. Work by [12], who used Tiwari and Das′ nanofluid model to model nanofluid flow in a right-angle trapezoidal enclosure, and [13], who used finite element methods to simulate nonlinear convective heat and mass transfer in a micropolar fluid-filled enclosure, are examples of additional studies into micropolar and nanofluid convection. [14] analyzed electrohydrodynamic (EHD)- induced natural convection in a micropolar fluid, demonstrating how electric fields interact with convection currents. [15] studied shallow cavity convection in micropolar fluids, noting that shallower enclosures exhibit different convection patterns compared to deeper ones. In order to take solid-fluid interactions into account, [16] used a local thermal non-equilibrium model to evaluate conjugate natural convection in a porous square enclosure filled with micropolar nanofluids. [17] emphasized the importance of localized magnetic field effects on vortex formation within lid-driven cavities, offering insights into how controlled magnetic fields can be utilized to manipulate flow structures. Similarly, [18] explored the coupling effects of Joule heating, porosity, and Lorentz forces in lid-driven enclosures, revealing complex interactions that influence heat transfer efficiency. [19] expanded on the influence of porous media by analytically investigating the interaction between two micropolar fluids within a rotating annulus. Their study highlighted the unique transport behaviors arising from micro-rotation interactions and porous confinement. Meanwhile, [20] focused on viscoplastic fluids but provided useful comparisons for natural convection studies in micropolar fluids, particularly within triangular enclosures.

The studies by [21] and [10] further underscored the significance of magnetic fields and radiation in shaping natural convection. [21] performed statistical and numerical assessments of MHD effects in hexagonal cavities, while [22] proposed a robust finite difference scheme for simulating MHD natural convection under radiative conditions in a quadrant-shaped enclosure. [23] offered additional insights by investigating the impact of multidirectional magnetic fields on convection patterns within square cavities featuring sinusoidal temperature distributions and heated/cold blocks. Their findings demonstrated how different magnetic field orientations can be used to optimize heat transfer processes.Dome-shaped enclosures (DSEs) are of particular interest due to their curved geometry, which affects the formation of convective cells and heat transfer efficiency. The presence of a magnetic field, in combination with thermal radiation and micropolar fluid properties, introduces additional complexities that require numerical modeling for a comprehensive understanding. Previous studies have primarily focused on rectangular and square enclosures, but investigations into curved enclosures such as domes remain limited. In this paper, the natural convection of an MHD micropolar fluid in a dome-shaped enclosure is investigated numerically. The enclosure's left and right walls are adiabatic, the top dome-shaped wall is kept cold,

and the bottom wall is kept at a steady temperature. The study focuses on how important dimensionless factors affect flow and heat transfer characteristics. These parameters include the Rayleigh number (Ra), Prandtl number (Pr), Hartmann number (Ha), micropolar parameter (K), and radiation parameter (Rd). To assess the impact of magnetic field orientation and strength, micropolar fluid characteristics, and radiative heat transfer on convection patterns, the governing equations−which are expressed in terms of the vorticity-stream function approach are numerically solved.

2. Mathematical Formulation

A two-dimensional computational dome-shaped enclosure occupied by micropolar fluid and a magnetic field is present in the y- direction. This is depicted in Figure 1. A perpendicular Lorentz body force is produced by the magnetic field, and the bottom wall of the dome-shaped enclosure is evenly heated while the other circular wall is isothermally cold. The thermal buoyancy term's density change is captured via the Boussinesq approximation. The electro-conductive micropolar fluid flow ignores viscosity dissipation, chemical reactions, and Joule heating while maintaining constant thermophysical characteristics.

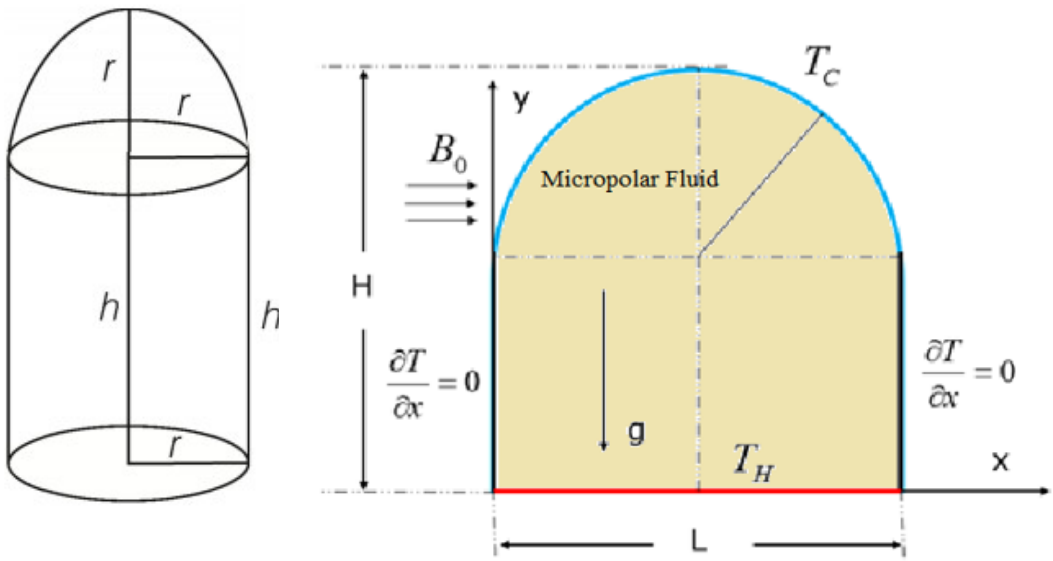

Figure 1: Computational Flow Geometry (a) 3D View (b) 2D Flow Geometry.

The following is an expression of the dimensional transport equations of conservation of momentum, mass, and energy based on the assumptions, using the references [24,25,26,27,28]: **Continuity Equation:**

$$\nabla \bullet u = 0 \tag{2.1}$$

Momentum Equation:

$$\rho \left(\frac{\partial u}{\partial t} + (u \bullet \nabla)\, u \right) = -\nabla P + \mu \nabla^2 u + \kappa \nabla^2 N + \rho g \beta \,(T - T_c) + J \times B \tag{2.2}$$

P – Pressure, μ - Dynamic viscosity, κ - coupling coefficient, N - microrotation vector, g - gravitational acceleration, β - thermal expansion coefficient, T - temperature, T_c - reference temperature, J - current density, B - magnetic field.

$$J = \sigma \,(E + u \times B)$$

$$\nabla \times B = \mu_0 J$$

Angular Momentum Equation:

$$\rho j\left(\frac{\partial N}{\partial t}+\left(u\bullet\nabla\right)N\right)=\gamma\nabla^2N--2\kappa N+\kappa\nabla\times u \tag{2.3}$$

γ - spin gradient, j - gyration parameter, κ - signify vortex viscosity.

Energy Equation:

$$\rho c_p\left(\frac{\partial T}{\partial t}+\left(u\bullet\nabla\right)T\right)=k\nabla^2T-\nabla\bullet q_r \tag{2.4}$$

c_p - specific heat capacity, q_r - radiative heat flux, k - thermal conductivity.

The cartesian form of the above modelling equations are as follows:

$$\frac{\partial u}{\partial x}+\frac{\partial v}{\partial y} \tag{2.5}$$

$$\rho\left(\frac{\partial u}{\partial t}+u\frac{\partial u}{\partial x}+v\frac{\partial u}{\partial y}\right)=\frac{-\partial p}{\partial x}+(\mu+k)\left(\frac{\partial^2u}{\partial x^2}+\frac{\partial^2u}{\partial y^2}\right)+k\frac{\partial N^*}{\partial y} \tag{2.6}$$

$$\rho\left(\frac{\partial v}{\partial t}+u\frac{\partial v}{\partial x}+v\frac{\partial v}{\partial y}\right)=\frac{-\partial p}{\partial y}+(\mu+k)\left(\frac{\partial^2v}{\partial x^2}+\frac{\partial^2v}{\partial y^2}\right)-\sigma B_0^2v-k\frac{\partial N^*}{\partial x}+\beta\rho g\left(T-T_c\right) \tag{2.7}$$

$$\rho j\left(u\frac{\partial N^*}{\partial x}+v\frac{\partial N^*}{\partial y}+\frac{\partial N^*}{\partial t}\right)+2kN^*=k\left(\frac{\partial v}{\partial x}-\frac{\partial u}{\partial y}\right)+\gamma\left(\frac{\partial^2N^*}{\partial x^2}+\frac{\partial^2N^*}{\partial y^2}\right) \tag{2.8}$$

$$\frac{\partial T}{\partial t}+u\frac{\partial T}{\partial x}+v\frac{\partial T}{\partial y}=\alpha_f\left(\frac{\partial^2T}{\partial x^2}+\frac{\partial^2T}{\partial y^2}\right)-\frac{1}{\left(\rho C_p\right)_f}\left(\frac{\partial q_x}{\partial\overline{x}}+\frac{\partial q_y}{\partial\overline{y}}\right) \tag{2.9}$$

where $(q_{rx},q_{ry})=\left(\frac{-4\sigma}{3k^*}\frac{\partial T^4}{\partial x},-\frac{4\sigma}{3k^*}\frac{\partial T^4}{\partial y}\right)$ The prescribed initial boundary conditions of present dome-shaped enclosure as follows:

At t=0 with for $0\leq x,y\leq L:0=u=T=v=N^*$

$T=T_c$, $N^*=n\frac{\partial v}{\partial n}$ at curved boundary

$T=T_h$, $N^*=n\frac{\partial v}{\partial x}$ at bottom wall

All boundaries

$$0=u=v \tag{2.10}$$

The equations (5) - (9) can be written dimensionless form with the help of below defined quantities: $\tau=\frac{t\alpha}{L^2},X=\frac{x}{L},Y=\frac{y}{L},(U,V)=\left(\frac{uL}{\alpha},\frac{vL}{\alpha}\right)$,

$$\theta=\frac{T-T_0}{T_h-T_c},T_0=\frac{T_h+T_c}{2},N=\frac{N^*L^2}{\alpha},P=\frac{L^2p}{\alpha^2\rho_f} \tag{2.11}$$

The non - dimensional form of interpreted governing equations are:

$$\frac{\partial U}{\partial X}=\frac{-\partial V}{\partial Y} \tag{2.12}$$

$$\frac{\partial U}{\partial\tau}+\frac{\partial P}{\partial X}=(1+K)\,Pr\left(\frac{\partial^2U}{\partial X^2}+\frac{\partial^2U}{\partial Y^2}\right)-\left(U\frac{\partial U}{\partial X}+V\frac{\partial U}{\partial Y}\right)+KPr\frac{\partial N}{\partial Y} \tag{2.13}$$

$$\frac{\partial V}{\partial\tau}+\frac{\partial P}{\partial Y}=(1+K)\,Pr\left(\frac{\partial^2V}{\partial X^2}+\frac{\partial^2V}{\partial Y^2}\right)-\left(U\frac{\partial V}{\partial X}+V\frac{\partial V}{\partial Y}\right)-KPr\frac{\partial N}{\partial X}-PrHa^2V+RaPr\theta \tag{2.14}$$

$$\frac{\partial N}{\partial\tau}+U\frac{\partial N}{\partial X}+V\frac{\partial N}{\partial Y}=\left(1+\frac{K}{2}\right)Pr\left(\frac{\partial^2N}{\partial X^2}+\frac{\partial^2N}{\partial Y^2}\right)-2KNPr+?KPr\left(\frac{\partial V}{\partial X}-\frac{\partial U}{\partial Y}\right) \tag{2.15}$$

$$\frac{\partial\theta}{\partial\tau}+U\frac{\partial\theta}{\partial X}+V\frac{\partial\theta}{\partial Y}=\left(1+\frac{4}{3}Rd\right)\left(\frac{\partial^2\theta}{\partial X^2}+\frac{\partial^2\theta}{\partial Y^2}\right) \tag{2.16}$$

Conditions on the boundaries of the computational domain are as follows:
On the enclosure walls (base and curved walls): $U = 0, V = 0$
Base wall: $\theta = 0.5, N = n\frac{\partial V}{\partial X}$.
Curved wall:

$$\theta = -0.5, N = -n\frac{\partial U}{\partial Y} \tag{2.17}$$

The other walls are adiabatic
The heat transfer rate (Local Nusselt number) along the base hot wall is measured the following

$$Nu = \frac{\partial \theta}{\partial Y} \tag{2.18}$$

The average value of the Nusselt number can be described as

$$Nu\_avg = \int_0^1 \frac{\partial \theta}{\partial Y} dX \tag{2.19}$$

3. Numerical methodology and code validation

The solution of the pressure based governing momentum equations are too complex due to this complexity; those equations are solved as follows:

$$U = \frac{\partial \psi}{\partial Y}, V = \frac{-\partial \psi}{\partial X} \tag{3.1}$$

$$\left(\frac{\partial^2 \psi}{\partial X^2} + \frac{\partial^2 \psi}{\partial Y^2}\right) = -\omega \tag{3.2}$$

$$\frac{\partial \omega}{\partial \tau} + U\frac{\partial \omega}{\partial X} + V\frac{\partial \omega}{\partial Y} = (1+K)\,Pr\left(\frac{\partial^2 \omega}{\partial X^2} + \frac{\partial^2 \omega}{\partial Y^2}\right)$$
$$-KPr\left(\frac{\partial^2 N}{\partial X^2} + \frac{\partial^2 N}{\partial Y^2}\right) - Ha^2 Pr\frac{\partial V}{\partial X} + Ra.Pr\frac{\partial \theta}{\partial X} \tag{3.3}$$

The numerical solution of modelled partial differential equations carried out with vorticity stream function algorithm. The development of the computational grid system is collocated grid. The equations that are being governed are discretized with a finite difference approximation of second order. For solving the discretized algebraic equations, the Linear Successive Over-Relaxation (LSOR) method is used, which is an iterative method. The numerical computation was proceeded until the meet the convergent criterion of each variable (i.e., ω, ψ, θ) which was $\sum_{i,j} \left|\Omega_{i,j}^{k+1} - \Omega_{i,j}^{k}\right| < 10^{-8}$, here k refers the iteration levels. The current numerical results provide strong support for the findings of [29] particularly regarding flow structure, thermal stratification, and heat transfer behavior. Using concise approaches for the pure stream function formulation of the incompressible viscous Navier-Stokes equations, Dutta et al. examined natural convective flow inside an enclosure. Their analysis focused on heat transfer within the enclosure at a Rayleigh number of 10^6, using air as the working fluid (Prandtl number = 0.71). This positive correlation not only validates our numerical model but also enhances our understanding of heat transfer characteristics in magnetized micropolar fluids. It effectively extends the scope of previous research to encompass more complex thermofluidic systems, encouraging further exploration in this area.

4. Results and Discussion

The influence of the emerging parameters magnetic number ($0 \leq \mathrm{Ha} \leq 30$), vortex viscosity parameter ($0 \leq \mathrm{K} \leq 5$), Rayleigh number ($10^3 \leq \mathrm{Ra} \leq 10^6$), Thermal radiation ($0 \leq \mathrm{Rd} \leq 5$) and on hydromagnetic micropolar fluid flow and heat distributions in a dome-shaped enclosure are discussed in this section and presented the contours plots for mentioned key parameters impact.
Figure 3 illustrates the impact of the Rayleigh number (Ra) on the streamlines, isotherms, and iso-microrotation contours, with Rd = 1, K = 1, Ha = 5, and Pr = 6.2. Increased circulation within the enclosure results from buoyancy-driven convection becoming more prevalent as Ra rises. Conduction

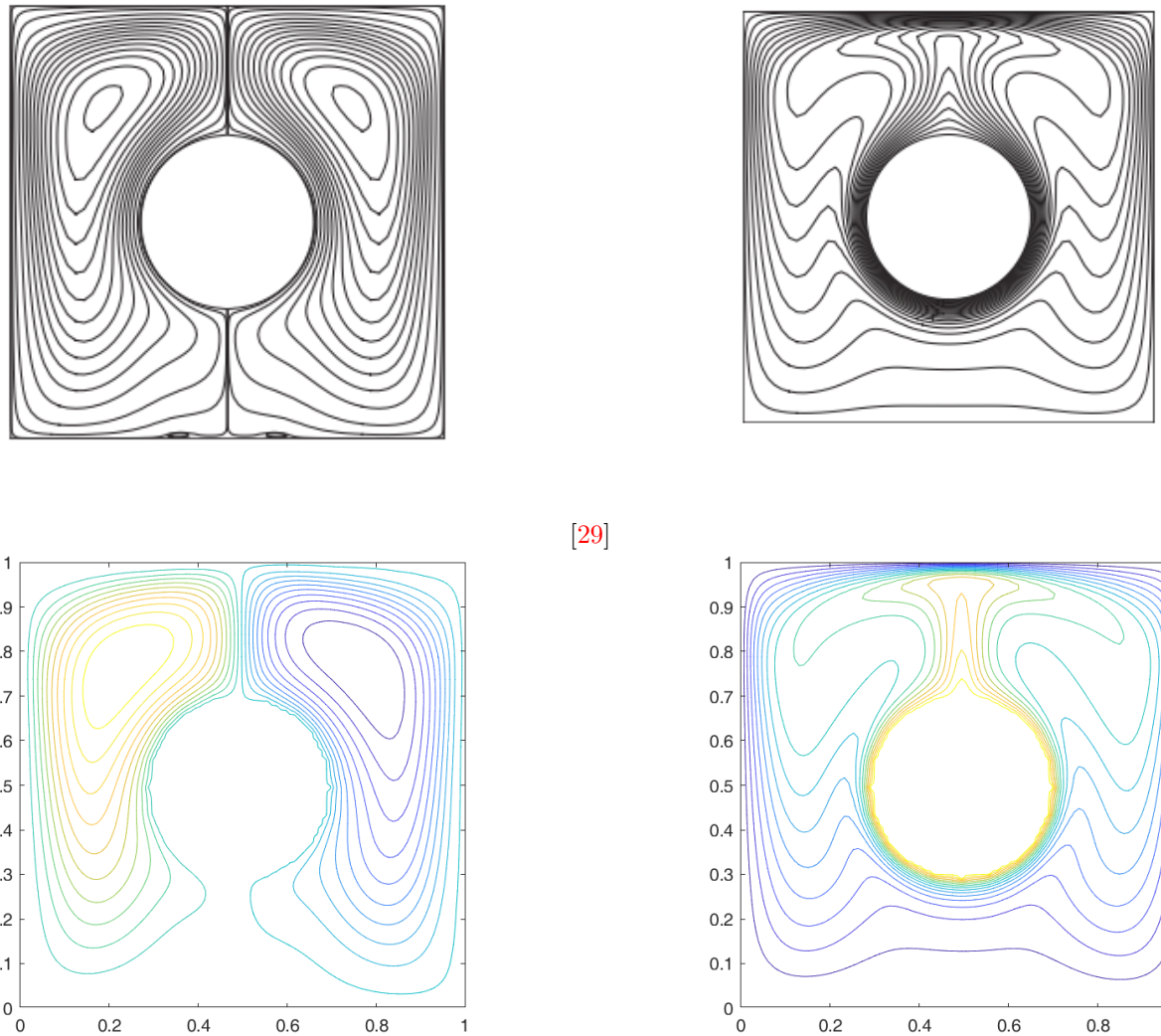

Figure 2: Comparison for the results of isotherms and stream lines.

takes over at lower Ra values, producing feeble convective motion and virtually parallel isotherms. As Ra increases, the streamlines indicate stronger convective cells, with flow intensification near the heated and cooled surfaces. This intensification leads to a more pronounced thermal gradient in the central region of the cavity. From a physical perspective, the increase in Ra signifies stronger thermal buoyancy effects, promoting heat transfer through convection rather than conduction. The iso-microrotation contours reveal a corresponding enhancement in rotational effects, showing higher microrotation values near the high-temperature gradient regions, particularly along the heated walls.

Figure 4 presents the effect of the Hartmann number (Ha) on streamlines, isotherms, and iso-microrotation, with Rd = 1, Ra = 10^5, K = 1, and Pr = 6.2. The presence of a magnetic field (characterized by Ha) introduces Lorentz forces, which suppress fluid motion and reduce convective activity. As Ha increases, the streamlines show a clear reduction in vortex intensity, leading to a more stabilized flow structure with weaker recirculation zones. The isotherms display a transition from a convective-dominant regime (low Ha) to a conduction-dominant regime (high Ha), where temperature gradients become more uniform due to flow suppression. The iso-microrotation contours indicate that

microrotation effects are also dampened as Ha increases, reducing rotational influences near the boundaries. Physically, the increasing Ha imposes a resistive force on the moving fluid due to electromagnetic damping, effectively weakening convective heat transfer.

Figure 5 examines the influence of the vortex-viscosity parameter (K) on streamlines, isotherms, and iso-microrotation, with Rd = 1, Ra = 10ˆ5, Ha = 5, and Pr = 6.2. The vortex-viscosity parameter controls the coupling between the velocity and microrotation fields, impacting the overall flow behavior and thermal transport characteristics. For low K values, the streamlines exhibit well-defined convective patterns, with strong circulatory motion driving heat transfer. As K increases, the flow structure becomes more diffused, with reduced intensity in recirculating regions. The isotherms become more distorted with lower K values due to stronger convective transport, whereas higher K leads to a more uniform temperature distribution, indicating increased resistance to convective effects. The iso-microrotation contours highlight the direct influence of K on rotational flow properties. Higher K values reduce microrotation gradients, indicating stronger viscous coupling effects that dampen localized rotational motion. From a physical standpoint, increasing K enhances the influence of vortex viscosity.

Figure 6 illustrates the variation of the local Nusselt number along the hot bottom wall for different Rayleigh numbers (Ra) while keeping Rd = 1, K = 1, Ha = 2. The Rayleigh number governs the buoyancy-driven convection, and its increase leads to enhanced convective heat transfer. Physically, at lower Ra values, conduction dominates, leading to a relatively uniform heat transfer rate along the bottom wall. As Ra increases, stronger convective currents develop, enhancing heat transfer near the walls due to the formation of thermal boundary layers. The local Nusselt number profile shows increased peaks at higher Ra, signifying greater thermal transport efficiency and increased flow circulation.

The local Nusselt number fluctuation along the heated bottom wall for various Hartmann numbers (Ha) while maintaining Rd = 1, K = 1, and Ra = 105 is shown in Figure 7. The intensity of the applied magnetic field, which modifies the flow structure by adding Lorentz forces that attenuate fluid velocity, is described by the Hartmann number. From a physical perspective, at low Ha values, buoyancy-driven convection dominates, resulting in pronounced peaks in the Nusselt number distribution. As Ha increases, the Lorentz force suppresses fluid movement, leading to reduced convective transport and a more uniform temperature distribution along the hot bottom wall. This results in a decline in the local Nusselt number values, indicating reduced heat transfer efficiency.

Figure 8 examines the influence of the vortex - viscosity parameter (K) on the local Nusselt number distribution, with Rd = 1 and Ha = 2. The parameter K governs the coupling between the velocity and microrotation fields in micropolar fluids. Physically, lower K values result in higher Nusselt numbers due to weaker microrotation effects, allowing stronger convective heat transfer. As K increases, the resistance to rotational effects becomes significant, reducing convective intensity and leading to a smoother Nusselt number profile with reduced peaks. This behavior confirms that increasing K enhances viscosity-related effects, dampening convective transport and decreasing thermal energy dissipation from the hot bottom wall.

Figure 9 shows how the local Nusselt number along the heated bottom wall is affected by the radiation parameter (Rd), when K = 1 and Ha = 2. The radiation parameter influences thermal radiation effects in the enclosure. At lower Rd values, conduction and convection dominate the heat transfer process, leading to a well-defined Nusselt number variation. As Rd increases, radiative heat transfer becomes significant, modifying the temperature field and reducing thermal gradients. This results in a more uniform Nusselt number distribution, indicating that radiative transport helps smooth temperature variations.

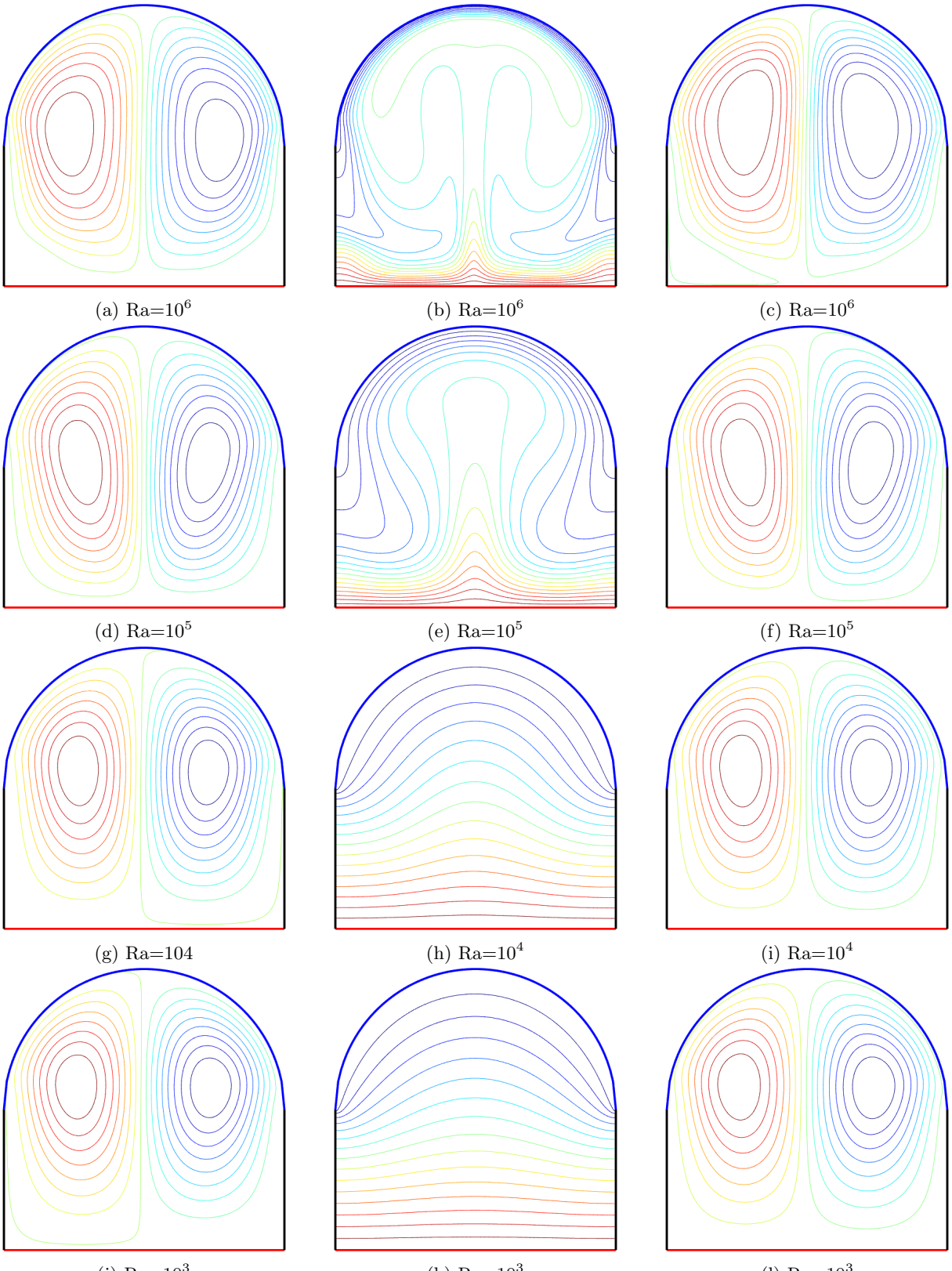

(a) Ra=10^6 (b) Ra=10^6 (c) Ra=10^6

(d) Ra=10^5 (e) Ra=10^5 (f) Ra=10^5

(g) Ra=104 (h) Ra=10^4 (i) Ra=10^4

(j) Ra=10^3 (k) Ra=10^3 (l) Ra=10^3

Figure 3: The influence of the Ra on streamlines, isotherms, and iso - microrotation with Rd =1, K=1, Ha = 5 and Pr = 6.2.

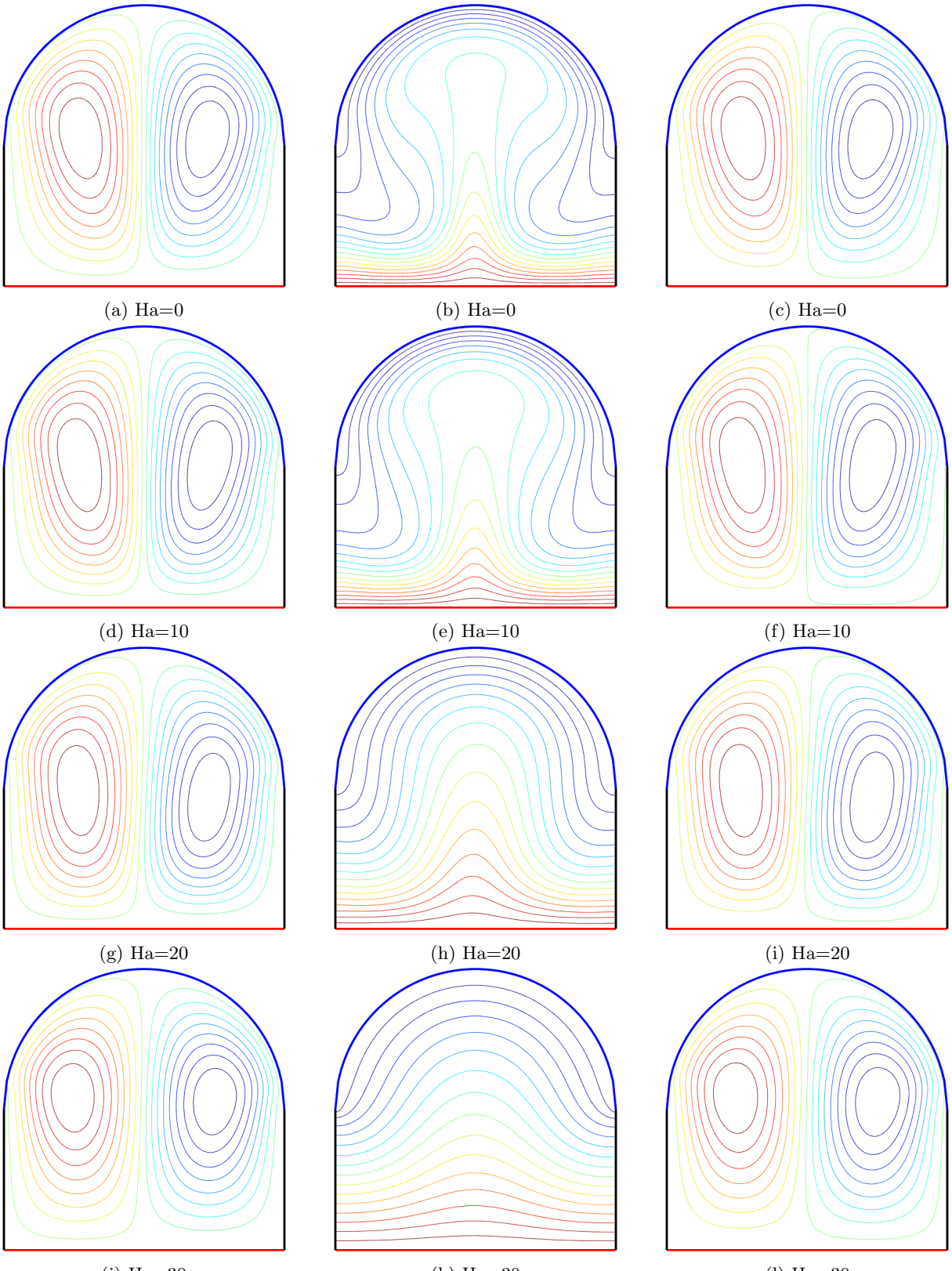

(a) Ha=0 (b) Ha=0 (c) Ha=0

(d) Ha=10 (e) Ha=10 (f) Ha=10

(g) Ha=20 (h) Ha=20 (i) Ha=20

(j) Ha=30 (k) Ha=30 (l) Ha=30

Figure 4: The influence of the Ha on streamlines, isotherms, and iso - microrotation with Rd =1, Ra=10^5, K = 1 and Pr = 6.2.

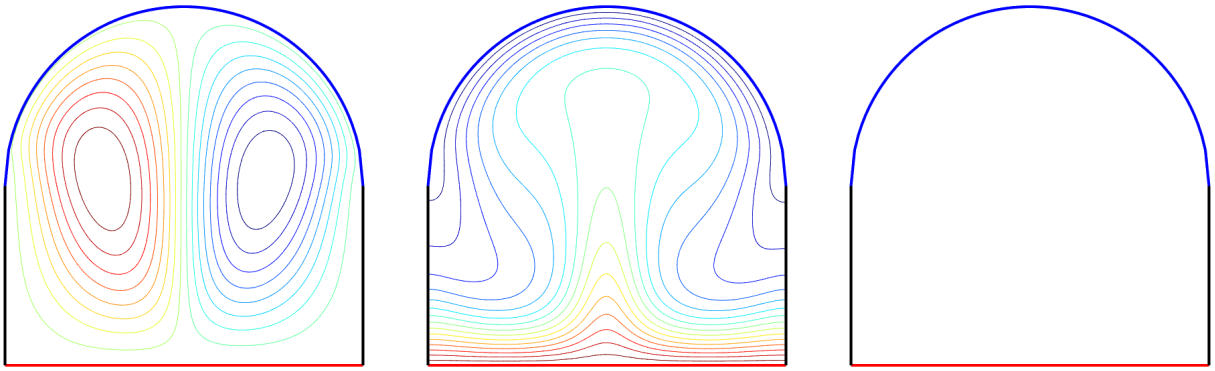

(a) K=0 (b) K=0 (c) K=0

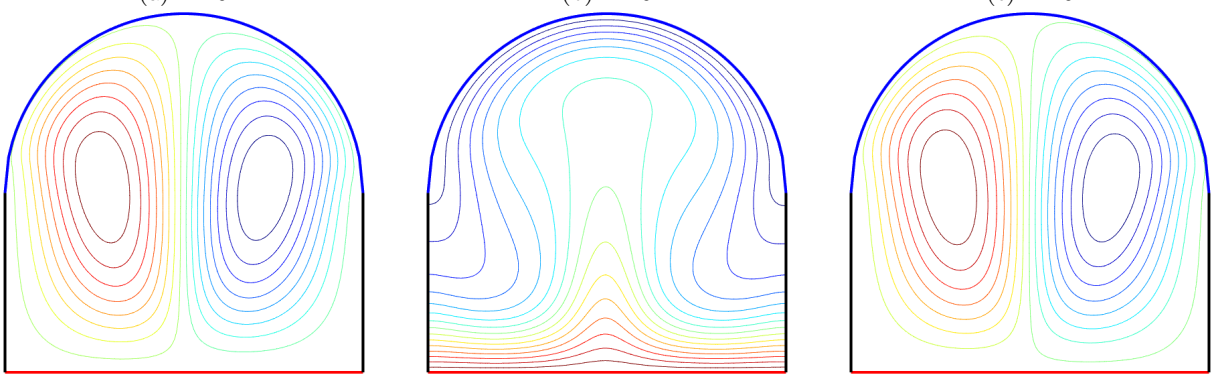

(d) K=0.5 (e) K=0.5 (f) K=0.5

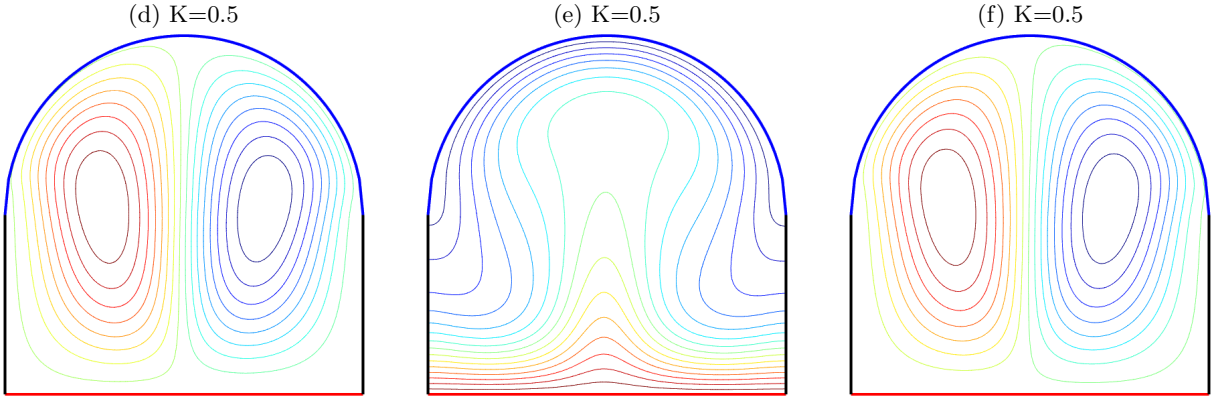

(g) K=1 (h) K=1 (i) K=1

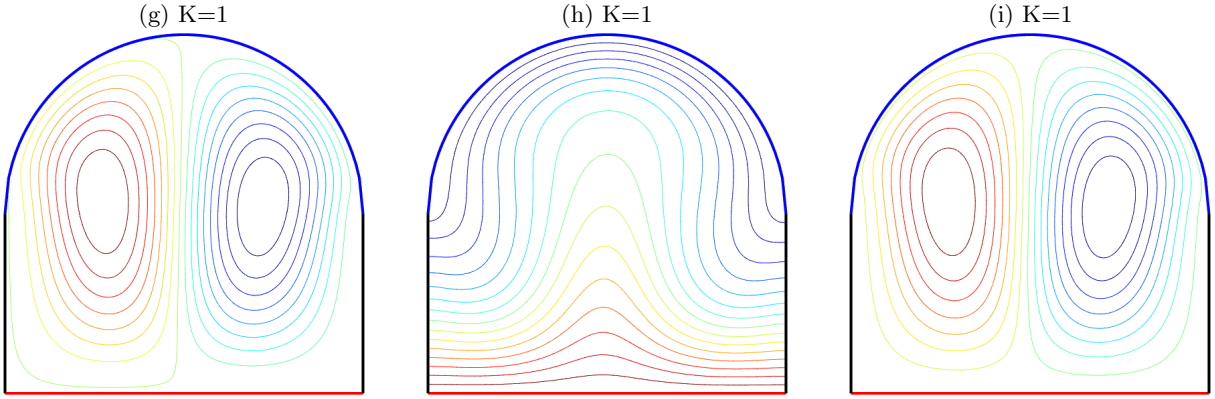

(j) K=2 (k) K=2 (l) K=2

Figure 5: The influence of the vortex - viscosity parameter K on streamlines, isotherms, and isomicrorotation with Rd =1, Ra=10^5, Ha = 5 and Pr = 6.2.

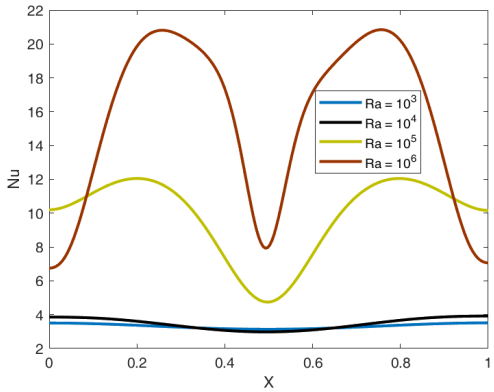

Figure 6: Local Nusselt number along the hot bottom wall with various Ra values with Rd = K=1, Ra = 10^5, Ha = 2.

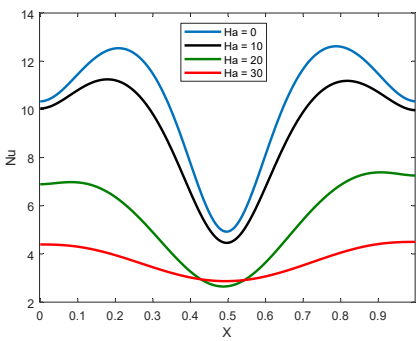

Figure 7: Local Nusselt number along the hot bottom wall with various Ha values with Rd = K=1, Ra = 10^6.

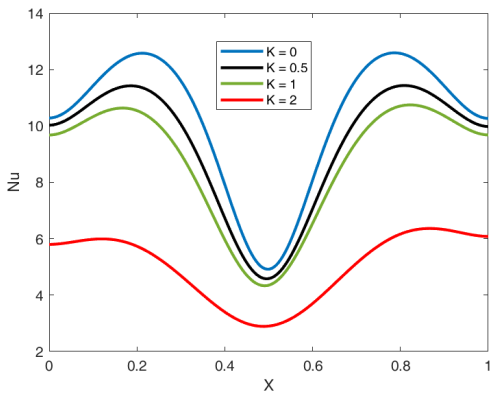

Figure 8: Local Nusselt number along the hot bottom wall with various K values with Rd =1, Ha = 2.

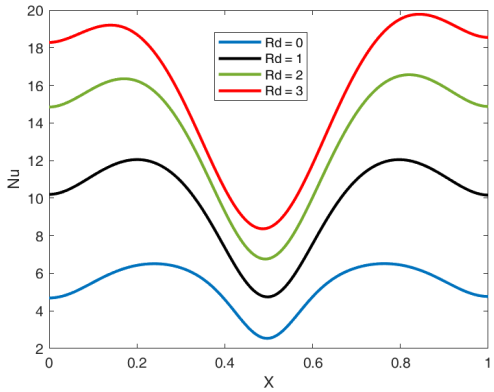

Figure 9: Local Nusselt number along the hot bottom wall with various Rd values with K=1, Ha = 2.

5. Conclusions

The effects of the radiation parameter (Rd), vortex-viscosity parameter (K), Rayleigh number (Ra), and Hartmann number (Ha) on heat transfer properties in a micropolar fluid system were thoroughly examined in this work. Two-dimensional magnetized micropolar fluid flow of natural convection in a dome-shaped enclosure has been quantitatively examined using the vorticity stream function technique. The analysis considers the impact of thermal radiation, Lorentz forces, vortex viscosity parameter and utilizes the finite difference method. Specifically, the dome-shaped enclosure consists a thermally equilibrium and electrically conducting of micropolar fluid. The momentum, energy, and mass conservation non-linear partial equations with defined wall boundary conditions of conventional micropolar fluid have been included. The computations have shown significant and noteworthy findings, which are listed below:

- Higher Ra enhances convective heat transfer, leading to increased thermal gradients and improved heat dissipation.
- Increasing Ha suppresses convection through Lorentz forces, reducing local Nusselt number variations and stabilizing heat transfer.
- Higher K weakens convective transport, decreasing heat dissipation efficiency and increasing viscosity-related effects.
- Larger Rd contributes to radiative heat transfer, leading to a more uniform temperature distribution and improved thermal stability.

These conclusions contribute to a more profound understanding of thermal convection within closed enclosures and suggest practical implications for optimizing the heat transfer systems' performance. Additionally, these findings are useful in designing effective thermal systems, including heat exchangers and fuel cells.

Declaration of Competing Interest: The authors state that none of their personal ties or known conflicting financial interests might have seemed to have influenced the work described in this study.
Conflicts of Interest: The authors say they have no conflicts of interest.
Data availability statement: No information related to the manuscript. Acknowledgments: The authors express their gratitude to the reviewers for their insightful remarks that have enhanced the study's clarity.

References

1. C. Perdikis and A. Raptis, *Heat transfer of a micropolar fluid by the presence of radiation*, Heat Mass Transf. 31, 381–382, (1996).

2. M. Nazeer, N. Ali, and T. Javed, *Natural convection flow of micropolar fluid inside a porous square conduit: effects of magnetic field, heat generation/absorption, and thermal radiation*, J. Porous Media. 21, no. 10, (2018).

3. M. Zadravec, M. Hriberšek, and L. Škerget, *Natural convection of micropolar fluid in an enclosure with boundary element method*, Eng. Anal. Bound. Elem. 33, no. 4, 485–492, (2009).

4. O. Aydın and I. Pop, *Natural convection in a differentially heated enclosure filled with a micropolar fluid*, Internat. J. Thermal Sci. 46, no. 10, 963–969, (2007).

5. T. H. Hsu, *Natural convection of micropolar fluids in a rectangular enclosure*, Internat. J. Engrg. Sci. 34, no. 4, 407–415, (1996).

6. O. Aydin and I. Pop, *Natural convection from a discrete heater in enclosures filled with a micropolar fluid*, Internat. J. Engrg. Sci. 43, no. 19–20, 1409–1418, (2005).

7. N. Ali, M. Nazeer, T. Javed, *et al.*, *A numerical study of micropolar flow inside a lid-driven triangular enclosure*, Meccanica. 53, 3279–3299, (2018).

8. T. Javed, Z. Mehmood, and M. A. Siddiqui, *Mixed convection in a triangular cavity permeated with micropolar nanofluid-saturated porous medium under the impact of MHD*, J. Braz. Soc. Mech. Sci. Eng. 39, 3897–3909, (2017).

9. V. Raja Rajeswari, K. Venkatadri, and V. Ramachandra Prasad, *Nanoparticle shape factor impact on double diffusive convection of Cu-water nanofluid in trapezoidal porous enclosures: A numerical study*, Numer. Heat Transfer, Part A. 2024, 1–20.

10. K. Venkatadri, K. V. N. Murthy, T. A. Bég, O. A. Bég, and S. Kuharat, *Numerical simulation of natural convection in a rectangular enclosure filled with porous medium saturated with magnetic nanofluid using Buongiorno's two-component model*, Canad. J. Chem. Eng. 2024, 1–22.

11. K. Venkatadri, O. A. Bég, P. Rajarajeswari, and V. R. Prasad, *Numerical simulation of thermal radiation influence on natural convection in a trapezoidal enclosure: Heat flow visualization through energy flux vectors*, Internat. J. Mech. Sci. 171, 105391, (2020).

12. K. Venkatadri, S. Fazuruddin, O. A. Bég, and O. Ramesh, *Natural convection of nanofluid flow in a porous medium in a right-angle trapezoidal enclosure: a Tiwari and Das' nanofluid model*, J. Taibah Univ. Sci. 17, no. 1, (2023).

13. R. Bhargava, S. Sharma, P. Bhargava, *et al.*, *Finite element simulation of nonlinear convective heat and mass transfer in a micropolar fluid-filled enclosure with Rayleigh number effects*, Internat. J. Appl. Comput. Math. 3, 1347–1379, (2017).

14. L. Samaei, H. M. Deylami, N. Amanifard, and H. Moayedi, *Numerical evaluation of using micropolar fluid model for EHD-induced natural convection heat transfer through a rectangular enclosure*, J. Electrostat. 101, 103372, (2019).

15. Z. Alloui and P. Vasseur, *Natural convection in a shallow cavity filled with a micropolar fluid*, Internat. J. Heat Mass Transf. 53, no. 13–14, 2750–2759, (2010).

16. S. A. M. Mehryan, M. Izadi, and M. A. Sheremet, *Analysis of conjugate natural convection within a porous square enclosure occupied with micropolar nanofluid using local thermal non-equilibrium model*, J. Mol. Liq. 250, 353–368, (2018).

17. S. Ahmad, K. Ali, T. Sajid, U. Bashir, F. L. Rashid, R. Kumar, *et al.*, *A novel vortex dynamic for micropolar fluid flow in a lid-driven cavity with magnetic field localization – A computational approach*, Ain Shams Eng. J. 15, no. 2, 102448, (2024).

18. H. Shahzad, Z. Li, T. Tang, and M. Kanwal, *Impact of micro-rotation on a double-diffusive radiative flow within a lid-driven enclosure featuring Joule heating, porosity and Lorentz forces*, J. Mol. Liq. 406, 125067, (2024).

19. S. Jaiswal and P. K. Yadav, *Analytical investigation of porous medium effects on the flow of two micropolar fluids in a rotating annulus*, Internat. J. Mod. Phys. B (2024), Article ID 2550111.

20. M. S. Aghighi, H. Masoumi, and A. Farsi, *Natural convection of viscoplastic fluids in a triangular enclosure*, Appl. Eng. Sci. 19, 100186, (2024).

21. M. S. Alam, M. N. Huda, M. M. Rahman, and M. M. Billah, *Statistical and numerical analysis of magnetic field effects on laminar natural convection heat transfer of nanofluid in a hexagonal cavity*, Internat. J. Thermofluids. 24, 100856, (2024).

22. K. Venkatadri, R. Saravana, O. A. Bég, *et al.*, *Robust finite difference scheme for the magnetohydrodynamics natural convection in a quadrant-shaped enclosure with radiation effect*, Eur. Phys. J. Plus. 139, 702, (2024).

23. M. Hamid, M. Usman, W. A. Khan, R. U. Haq, and Z. Tian, *Natural convection and multidirectional magnetic field inside a square shaped cavity with sinusoidal temperature and heated/cold blocks*, Internat. Commun. Heat Mass Transf. 152, 107291, (2024).

24. A. Mahdy, S. E. Ahmed, and M. A. Mansour, *Entropy generation for MHD natural convection in enclosure with a micropolar fluid saturated porous medium with Al_2O_3–Cu water hybrid nanofluid*, Nonlinear Anal.: Model. Control. 26, no. 6, 1123–1143, (2021).

25. N. Ali, M. Nazeer, and T. Javed, *Finite element simulations of free convection flow inside a porous inclined cavity filled with micropolar fluid*, J. Porous Media. 24, no. 2, (2021).

26. Z. A. Raizah, S. E. Ahmed, D. Alrowaili, M. A. Mansour, and Z. Morsy, *Magnetic micropolar nanofluids flow in double lid-driven enclosures using two-energy equation model*, Heat Transfer. 50, no. 3, 2743–2763, (2021).

27. C. Sivarami Reddy, V. Ramachandra Prasad, and K. Jayalakshmi, *Numerical simulation of natural convection heat transfer from a heated square cylinder in a square cavity filled with micropolar fluid*, Heat Transfer. 50, no. 6, 5267–5285, (2021).

28. S. M. Seyyedi, M. Hashemi-Tilehnoee, E. P. Del Barrio, A. S. Dogonchi, and M. Sharifpur, *Analysis of magneto-natural-convection flow in a semi-annulus enclosure filled with a micropolar-nanofluid; a computational framework using CVFEM and FVM*, J. Magn. Magn. Mater. 568, 170407, (2023).

29. S. Dutta, P. Kumar, and J. C. Kalita, *Streamfunction-velocity computation of natural convection around heated bodies placed in a square enclosure*, Internat. J. Heat Mass Transf. 152, 119550, (2020).

Nomenclature

Symbol	Description	Symbol	Description
B_0	*Magnetic field*	P	*Pressure*
C_P	*Specific heat*	t	*Time*
Ha	*Hartmann number*	T	*Temperature*
g	*gravitational acceleration*	N^*	*Dimensionless micro rotation angular velocity*
Pr	*Prandtl number*	(U, V)	*Dimensionless velocity component in X, Y-direction*
N	*Dimensional micro rotation angular velocity*	(x, y)	*Cartesian coordinate in horizontal and vertical direction*
k	*Vortex viscosity parameter*	Rd	*Thermal radiation*
L	*Length of the enclosure*	H	*Height of the enclosure*
Ra	*Rayleigh number*		*Greek letters*
K	*Dimensionless vortex viscosity*	μ	*Dynamic viscosity*
(X, Y)	*Dimensionless vortex viscosity*	ρ	*Fluid density*
(u, v)	*Dimensional component of fluid velocity in x, y-direction*	γ	*Spin-gradient viscosity*
T_c	*Temperature at cold wall*	τ	*Non-dimensional time*
T_h	*Temperature at hot wall*	α	*Thermal diffusivity*
Nu	*Local Nusselt number*	θ	*Non-dimensional temperature*

Gandrakota Kathyayani,
Professor Department of Applied Mathematics,
Yogi Vemana University, Kadapa, A.P, India - 516005.
E-mail address: kathyagk@yvu.edu.in

and

Siddamsetti Maheswari,
Research Scholar Department of Applied Mathematics,
Yogi Vemana University, Kadapa, A.P, India - 516005.
E-mail address: maheswarisiddamsetti@gmail.com

and

Gattu Venkata Ramudu,
Research Scholar Department of Applied Mathematics,
Yogi Vemana University, Kadapa, A.P, India - 516005.
E-mail address: ramudu6594@gmail.com